PAPER

Check for updates

[Fe(bpy)₃]²⁺-based porous organic polymers with boosted photocatalytic activity for recyclable organic transformations†

Hong-Kun Liu,[a] Yi-Fei Lei,[a] Peng-Ju Tian,[b] Hui Wang,[a] Xin Zhao,[b] Zhan-Ting Li [ID] *[a] and Dan-Wei Zhang [ID] *[a]

Three rigid metal porous organic polymers (POPs) based on an iron(ɪɪ) complex are prepared from the condensation reactions of an octahedral [Fe(bpy)₃]²⁺-cored hexaaldehyde and three rod-like aromatic diamines. The POPs have been studied as the first series of earth-abundant metal complex-connected photocatalysts for heterogeneous visible light-driven oxidation of benzyl halides and enantioselective α-alkylation of aldehydes. Both yields and enantioselectivities of the reactions catalyzed by one of the POPs, which possesses the largest porosity, rival or even surpass those of the reactions homogeneously catalyzed by control [Fe(bpy)₃]²⁺ complexes. Moreover, POP catalysts are highly stable and exhibit a considerable activity after recycling 10 times.

Introduction

In the past two decades, visible light photoredox catalysis of organic transformations has received great attention due to its mild reaction conditions and the potential of harvesting solar energy for chemical transformations.[1–12] Currently, there are two major kinds of photosensitizers, *i.e.*, transition metal complexes and organic dyes,[13–20] which can efficiently mediate single-electron transfer processes with organic substrates upon photoexcitation with visible light. In the first category, complexes of ruthenium and iridium with various pyridine ligands have been most widely investigated for various organic transformations.[1–13] However, both metals are precious and have very low abundance ($\sim 10^{-7}$) in Earth's crust. Thus, chemists have a long-standing interest in photoactive molecular complexes made from abundant elements,[21–29] particularly the iron element that has very high abundance (4.7%) in the crust and is much less expensive,[30–32] even though iron complexes typically have a short-lived excited state that does not favor the initiation of electron transfer-mediated organic reactions. In 2015, Cozzi, Ceroni and co-workers reported that [Fe(bpy)₃]²⁺

(bpy: 2,2′-bipyridine) can enable photocatalytic enantioselective alkylation of aldehydes with various α-bromocarbonyl compounds.[33] With [Fe(phen)₃]²⁺ (phen: 1,10-phenanthroline) as a photocatalyst, Collins and co-workers realized the oxidative cyclization of triaryl and diarylamines into their corresponding carbazoles,[34] whereas Kang and co-workers achieved the cyclo-addition reactions of alkene radical cations with diazo compounds to afford cyclopropanes and single-electron oxidation and α-deprotonation of tertiary anilines to yield α-amino-alkyl radicals, which couple with electrophilic reagents to form tetrahydroquinolines.[35,36] All the reactions are carried out in a homogeneous manner. Further development of heterogeneous methodologies for recyclable utilization of catalysts would not only lower the costs of both the metal and ligand, but would also enhance the environmentally benign feature of iron-based catalysts. To the best of our knowledge, such methodologies have not been reported for complex catalysts made from iron and other earth-abundant transition metals.

Porous organic polymers (POPs) represent a class of highly cross-linked and synthetically accessible conjugated materials with inherent porosity that enables a variety of functions or applications.[37–42] One of the most promising applications of POPs has been the development of recyclable, heterogeneous catalysts for efficient organic transformations.[43–45] In this category, rigid, well-defined ruthenium and iridium complexes have been incorporated into or appended to the frameworks of POPs for the catalysis of a large number of organic reactions under visible-light irradiation.[46–57] Replacement of the precious metal complexes with iron complexes may further reduce the cost of the heterogeneous catalysts by maintaining the recyclability of the corresponding POPs. We herein describe the synthesis of three highly stable [Fe(bpy)₃]²⁺(bpy: 2,2′-bipyridine)-based,

[a]*Department of Chemistry, Shanghai Key Laboratory of Molecular Catalysis and Innovative Materials, Fudan University, 2205 Songhu Lu, Shanghai 200438, China. E-mail: ztli@fudan.edu.cn; zhangdw@fudan.edu.cn*

[b]*Key Laboratory of Synthetic and Self-Assembly Chemistry for Organic Functional Molecules, Shanghai Institute of Organic Chemistry, Chinese Academy of Sciences, 345 Lingling Lu, 200032, China*

This journal is © The Royal Society of Chemistry 2021

J. Mater. Chem. A, 2021, 9, 6361–6367 | **6361**

noble-metal-free porous organic polymers (**Fe-POP-1–3**) from the condensation reaction of a $[Fe(bpy)_3]^{2+}$-derived hexaaldehyde and three rod-like aromatic diamines. We demonstrate that the three coordination polymers could be applied to visible-light-driven oxidation of benzyl halides and enantioselective α-alkylation of aldehydes with high recyclability of up to ten times. In particular, the $[Fe(bpy)_3]^{2+}$ unit in heterogeneous **Fe-POP-1**, which possesses the largest pore aperture, exhibits comparable or even higher catalytic activity for both reactions as compared with homogeneous control complexes.
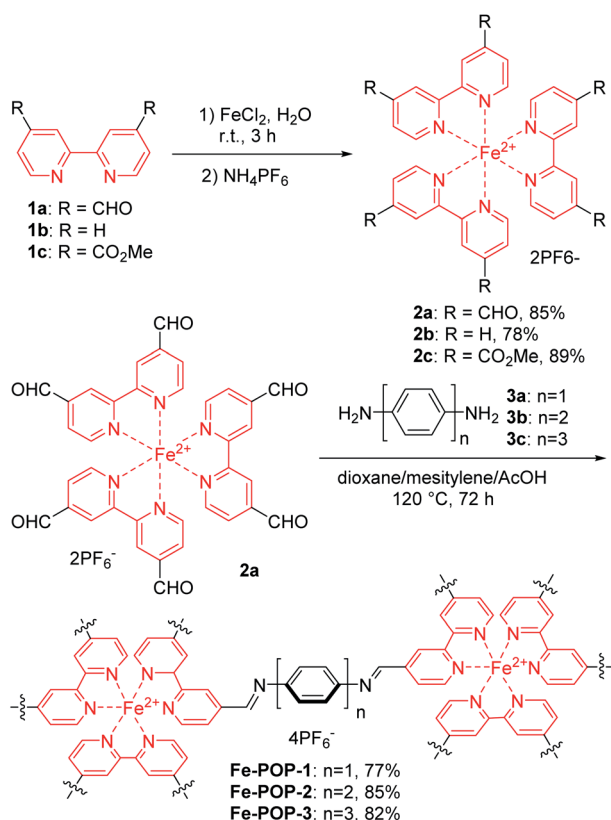
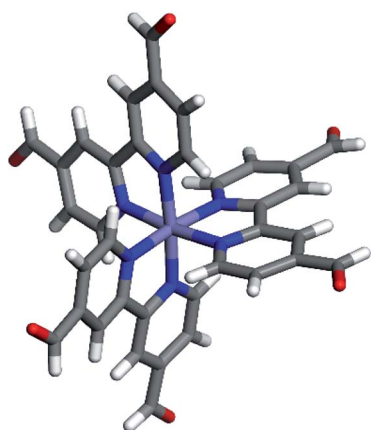Scheme 1 The synthesis of complexes **2a–c** and POPs **Fe-POP-1–3**.

Fig. 1 Crystal structure of complex **2a**.

Results and discussion

The synthetic routes for **Fe-POP-1–3** are shown in Scheme 1. The key intermediate, iron(II) complex hexaaldehyde **2a**, was synthesized from the reaction of **1a** with ferrous chloride in deionized water. Subsequently, iron(II) complex **2a** was treated with **3a–c** in the mixture of 1,4-dioxane/mesitylene or 1,2-dichlorobenzene/isopropanol at 120 °C for 3 days to afford **Fe-POP-1–3**, respectively. As control complexes, iron(II) complexes **2b** ($Fe(bpy)_3(PF_6)_2$) and **2c** were also prepared from the reaction of ferrous chloride with bipyridine ligand **1b** or **1c**. Single crystals were obtained by diffusing diethyl ether into the saturated solution of **2a** in acetonitrile. Its X-ray diffraction structure confirmed the octahedral feature of the complex (Fig. 1). Thus, its condensation with rod-like monomers **3a–c** was expected to afford rigid $[Fe(bpy)_3]^{2+}$-connected POPs **Fe-POP-1–3**, which could lead to a short-range *pcu* topological structure through an ideal condensation process. All the polymers were insoluble in common solvents including water, dimethyl sulfoxide (DMSO), *N,N*-dimethylformamide (DMF), acetone and acetonitrile. In contrast, control complexes **2b** and **2c** were highly soluble in the above organic solvents. Thermogravimetric analyses (TGA) revealed that polymers **Fe-POP-1–3** were stable up to 400 °C (15% weight loss) (Fig. S1, ESI†).

Fourier transform infrared spectroscopy of **Fe-POP-1–3** did not exhibit the absorption of the C=O stretching vibration of compound **2a** at 1707 cm^{-1} or the absorption of the N–H stretching vibration around 3350 cm^{-1} of compounds **3a–c** (Fig. S2–S4, ESI†), respectively, which indicated that the monomers were consumed nearly completely in the condensation reactions. The solid-state UV-vis spectra of the three POPs (Fig. S5, ESI†) displayed a wide range of UV-vis absorptions, whereas the fluorescence spectra exhibited two emissions centred around 486 and 530 nm (Fig. S6, ESI†), suggesting tremendous photo-activity and potential photocatalysis. Scanning electron microscope (SEM) images showed the formation of amorphous structures (Fig. S7–S9, ESI†), and powder X-ray diffraction (PXRD) profiles did not exhibit assignable peaks, which also suggested the amorphous feature (Fig. S10, ESI†). Energy dispersive X-ray spectroscopy (EDS) supported the existence of Fe, C, N, P, and F elements for all three polymers (Fig. S11–S13, ESI†), whereas their X-ray photoelectron spectroscopic (XPS) profiles further confirmed the composition of the above elements (Fig. 2). The binding energy of $2p_{3/2}$ of the Fe element of the three polymers (708.3, 709.8, and 709.4 eV, respectively) was all close to the value of FeO (709.1–709.6 eV) (Fig. 2b), but far from that of Fe_2O_3 (711.3–711.9 eV), indicating that no valence change occurred for the Fe element during the polymerization. The profiles also showed the peak of the O element, which could be attributed to solvent molecule adsorption by the materials and/or the oxidation of partial Fe^{2+} complexes to Fe^{3+} complexes.[46,55,56] Inductively coupled plasma atomic emission spectrometric (ICP-AES) analysis revealed that the three polymers had an Fe content of 4.47%, 3.90%, or 3.29%, which was close to their respective calculated values (4.66%, 3.92%, and 3.38%) after quantitative condensation,
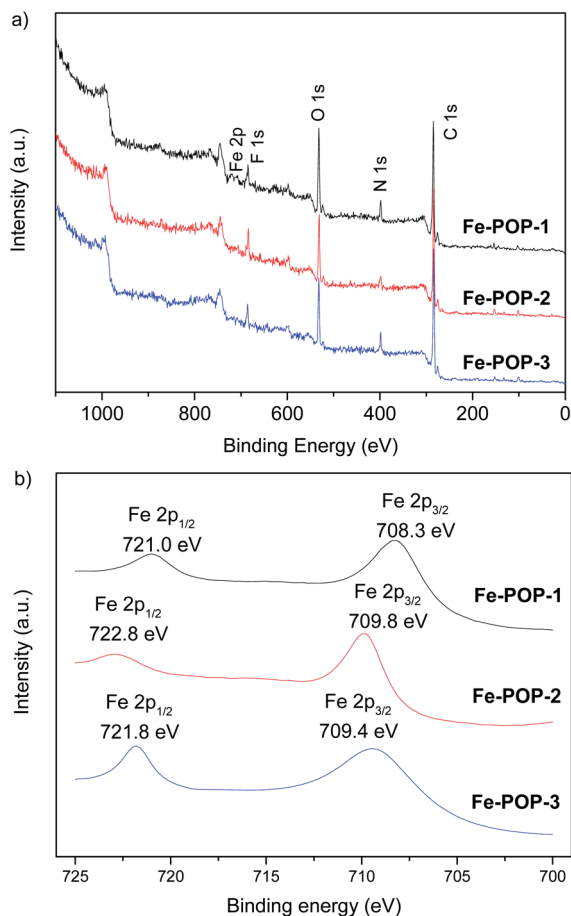
6362 | *J. Mater. Chem. A*, 2021, **9**, 6361–6367

This journal is © The Royal Society of Chemistry 2021

Fig. 2 (a) The XPS survey spectra and (b) the Fe 2p spectra of polymers **Fe-POP-1–3**.

which also supported that the complex did not decompose during polymerization and thus no Fe loss occurred due to the decomposition of the complex.

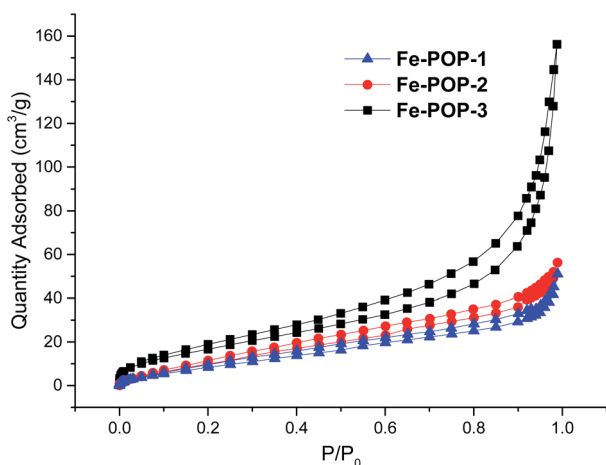The permanent porosity of **Fe-POP-1–3** was investigated by nitrogen sorption measurements at 77 K. Their Brunauer–

Fig. 3 N₂ adsorption and desorption isotherms of polymers **Fe-POP-1–3** at 77 K.

Emmett–Teller (BET) surface area were determined to be 39, 49 and 65 $m^2 g^{-1}$, respectively (Fig. 3). The existence of the optical isomers of the $[Fe(bpy)_3]^{2+}$ complexes and PF_6^- counterions may account for the low or modest surface area, as revealed for ruthenium or iridium complex-based POPs.[46,52,55] The surface area increased with the elongation of the linkers in the polymers, which implied that **Fe-POP-3** might exhibit the highest catalytic efficiency.
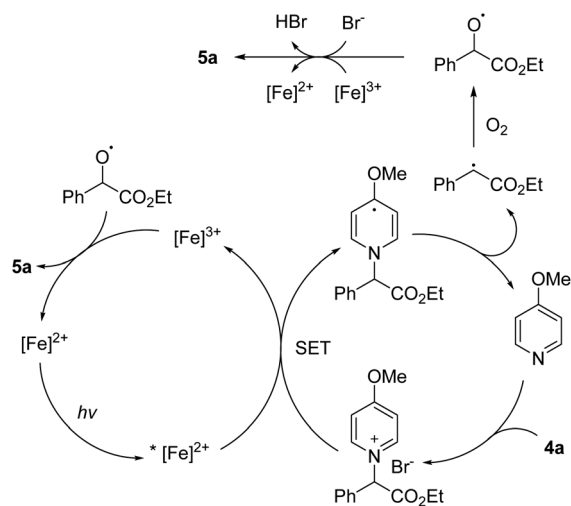
The potential of **Fe-POP-1–3** for heterogeneous visible-light-driven photocatalysis of organic transformations was then explored. The oxidation reaction of benzyl halides, which affords the corresponding phenyl carbonyl compounds, was investigated firstly. Previously, Jiao and co-workers realized this oxidation process homogeneously in *N,N*-dimethyl acetamide (DMAc) with $Ru(bpy)_3Cl_2$ as a photosensitizer.[58] With air O_2 as the oxidant, this reaction provides a one-step method of transforming benzyl halides to the corresponding phenyl carbonyl compounds. Cheng and Zhang and co-workers also utilized metal–organic framework-loaded $[Ru(bpy)_3]Cl_2$ to photocatalyze this reaction heterogeneously.[59] We first studied the oxidation of compound **4a** to produce **5a** with **Fe-POP-1–3** as heterogeneous photocatalysts under the conditions used with $[Ru(bpy)_3]Cl_2$ as a homogeneous photocatalyst.[58] The results are summarized in Table 1. All three POPs catalyzed the reaction and **5a** was obtained in 63%, 74% or 90% yield (entries 1–3), respectively. Under the identical conditions, controls **2b** and **2c** also catalyzed the reaction homogeneously to yield **5a** in 53% or 64% yield (entries 4 and 5). Given the amorphous nature of the POPs,

Table 1 Optimization of the photocatalytic oxidation reaction of benzyl halide **4a**[a]
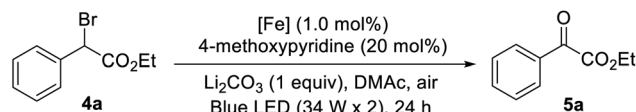
Entry	Catalyst (1.0 mol%)	Solvent	Yield[b] (%)
1	**Fe-POP-1**	DMAc	63
2	**Fe-POP-2**	DMAc	74
3[c]	**Fe-POP-3**	DMAc	90
4[c]	**2b**	DMAc	53
5[c]	**2c**	DMAc	64
6[d]	—	DMAc	16
7[e]	**Fe-POP-3**	DMAc	64
8[f]	**Fe-POP-3**	DMAc	79
9	**Fe-POP-3**	DMF	65
10	**Fe-POP-3**	MeCN	29
11	**Fe-POP-3**	ⁱPrOH	41
12	**Fe-POP-3**	THF	39
13	**2c**	ⁱPrOH	34
14	**2c**	THF	28

[a] Reaction conditions: **4a** (1.0 mmol), [Fe] (0.01 mmol), cocatalyst 4-methoxypyridine (0.2 mmol), Li_2CO_3 (1.0 mmol), solvent (5 mL) under air at 25 °C, irradiation with two 34 W blue LED lights at a distance of 8 cm for 24 h. [b] Yield determined by GC using *n*-dodecane as the internal standard. [c] Average value of the three reactions. [d] Without the addition of the metal catalyst. [e] 15 mol% 4-methoxypyridine was used. [f] Na_2CO_3 used as the base.

This journal is © The Royal Society of Chemistry 2021

J. Mater. Chem. A, 2021, **9**, 6361–6367 | **6363**

Scheme 2 Proposed mechanism for the photocatalytic oxidation of **4a** to **5a** with polymers **Fe-POP-1–3** as heterogeneous catalysts.

it is reasonable to assume that not all of the $[Fe(bpy)_3]Cl_2$ units of the POPs could be reached by the substrate molecules. Thus, the fact that **Fe-POP-2** and **Fe-POP-3** realized higher yields of **5a** than **2b** or **2c** should be attributed to the cooperative effect of the $[Fe(bpy)_3]Cl_2$ units, which, in an ideal structure, could form a cubic cage to facilitate the oxidation of the substrate. In the absence of the catalysts, **5a** was obtained in 16% yield (entry 6). Visible light irradiation was indispensable for the reaction, because removing the lamps during the reaction nearly completely stopped the reaction (Fig. S14, ESI†). As **Fe-POP-3** exhibited obviously higher photocatalytic activity, we further studied the effect of different reaction conditions on the reaction of this POP. It was revealed that decreasing the amount of 4-methoxypyridine cocatalyst caused significant reduction of the yield (entry 7), whereas using Na_2CO_3 as a base also led to a slight decline of the yield (entry 8). The oxidation reaction could also take place in DMF, MeCN, iso-PrOH or THF (entries 9–12), but the yield of **5a** decreased significantly. Although the yields were all lowered, with iso-PrOH or THF as solvent, **Fe-POP-3** could also afford a higher yield of **5a** than control complex **2c**, which was insoluble in the two solvents and thus should function in a heterogeneous manner (entries 11–14), which further illustrated the importance of the porosity of the POPs in boosting their catalytic activity. ICP-AES experiments revealed that the contents of Ir, Ru, Pd or Rh in Fe-POPs were less than 0.02 ppm, which supported that the catalysis was not caused by these rare transition metals possibly present in the POPs. We thus proposed that this heterogeneous photocatalytic oxidation of **4a** to **5a** proceeded through the mechanism established for the same reaction with $[Ru(bpy)_3]Cl_2$ as a homogeneous photocatalyst (Scheme 2).[57]

The recyclability of **Fe-POP-3** was also investigated for the above oxidation reaction. The solid catalyst was isolated by centrifugation, washed with deionized water and DMAc and then reused in a fresh reaction solution. The reaction yield of **5a** gradually decreased (Fig. 4a). However, after ten cycles, **5a** was
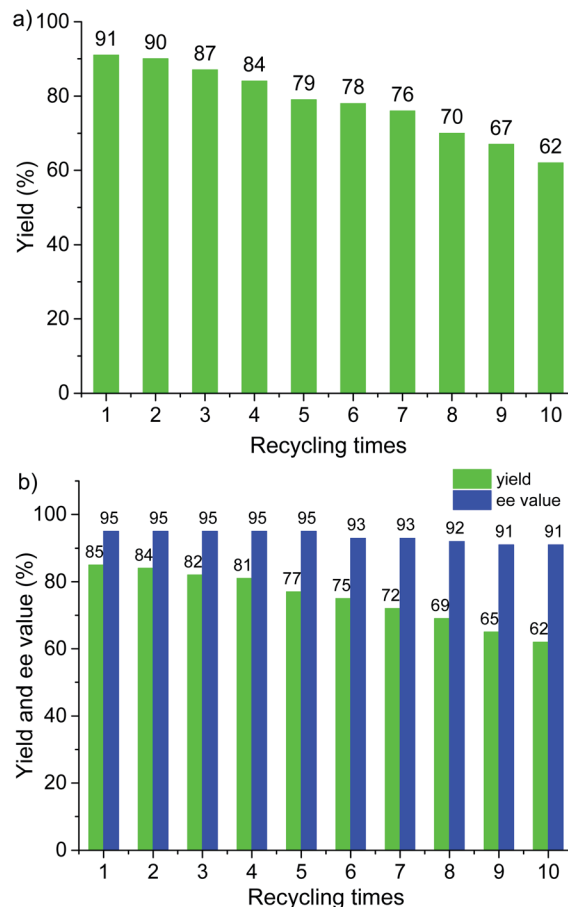
Fig. 4 (a) Recyclability of **Fe-POP-3** in the oxidation reaction of **4a** (2.0 mmol) to form **5a**. (b) Recyclability of **Fe-POP-3** in the reaction of **6a** and **7a** to form **9a**.
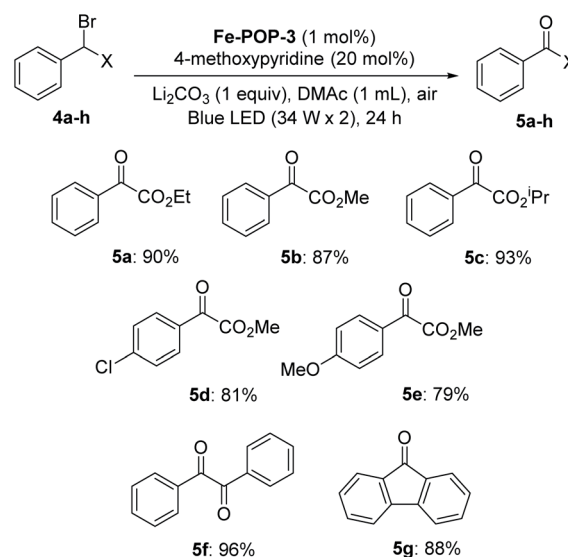
Scheme 3 Substrate scope of **Fe-POP-3** catalyzed oxidation of benzyl halides **4a–h** to form the corresponding phenyl carbonyl compounds **5a–h**. The yield represented is the isolated yield.

6364 | *J. Mater. Chem. A*, 2021, **9**, 6361–6367

This journal is © The Royal Society of Chemistry 2021

still obtained in 62% yield, which well reflected the high stability of the catalyst. The gradual decrease of the yield might be caused by the loss and decomposition of the catalyst as well as metal leaching during the process.

The above reaction conditions (Table 1) were then applied to a series of 2-bromo-2-phenylacetates (**4b–e**) (Scheme 3). **Fe-POP-3** was chosen as the photocatalyst because of its highest photocatalytic activity. All the reactions gave rise to the corresponding ketone derivatives (**5b–e**) in high to excellent yields (79–93%), which showed high tolerance of the ester groups as well as the substituents on the benzene ring. The above reaction conditions could also be applied to 2-bromo-1,2-diphenylethan-1-one **4f**, which gave rise to benzil **5f** in 96% yield. Under the identical reaction conditions, 9-bromofluorene **4g** was also oxidized to afford fluorenone **5g** in 88% yield.

Visible-light-driven enantioselective α-alkylation of aldehydes represents a mild and efficient transformation for asymmetric C–C bond formation. This reaction was first reported by Nicewicz and MacMillan using Ru(bpy)$_3$Cl$_2$ (0.5 mol%) as a homogeneous photocatalyst and the MacMillan catalyst chiral imidazolidinone **8** as a chiral-organocatalyst.[60] Ceroni and Cozzi described that catalytic amounts (2.5 mol%) of the [Fe(bpy)$_3$]Br$_2$ complex can help realize this reaction to produce the corresponding products with comparable yields and enantioselectivities.[33] We thus further explored the capability of **Fe-POP-1–3** as heterogeneous photocatalysts for this transformation. We first studied the reaction of **6a** and **7a** in the presence of catalytic amounts of **Fe-POP-1–3** ([Fe]: 1 mol%), **8** (20 mol%) and 2,6-lutidine (2 equiv.) in DMF (Table 2). The

coupling product **9a** was produced in 23%, 53% and 85% yields (entries 1–3, Table 2), respectively. These results were consistent with those of the above oxidation reaction, showing that large porosity of the POPs favored the photocatalytic process. Further increase of **Fe-POP-3** did not improve the yield of **9a**, whereas in the presence of 0.5 mol% ([Fe]) amount of **Fe-POP-3**, **9a** could be obtained in 76% yield (entries 4 and 5). Again, we found that visible light irradiation was also indispensable for this reaction (Fig. S15, ESI†). The photocatalyst also worked well in THF to allow for the generation of **9a** in 80% yield (entry 6), but in iso-propanol, the yield of **9a** was substantially lowered (entry 7). Control photocatalyst **2b** also efficiently catalyzed the reaction in DMF to afford **9a** in 83% yield in a heterogeneous manner (entry 8). Another control **2c** was also soluble in DMF, but did not exhibit photocatalytic activity (entry 9). Thus, once again, the heterogeneous photocatalyst **Fe-POP-3** can realize a catalytic activity that rivals or even surpasses that of a homogeneous one. With iso-propanol as solvent, in which both **2b** and **2c** were insoluble, the two photocatalysts allowed the formation of **9a** in 21% and 7% yields (entries 10 and 11), respectively.

From the reaction of **6a** and **7a**, **9a** was obtained with high enantioselectivity (95% ee), which was comparable with that (93% ee) obtained under the homogeneous catalysis of Fe(bpy)$_3$Br$_2$.[33] We then applied the above optimized reaction conditions to the reactions between aldehydes **6a** and **6b** and 2-

Table 2 Optimization of the photocatalytic enantioselective reaction of aldehyde **6a** and bromide **7a** to afford **9a**

Entry	Catalyst (mol%)	Solvent	Yield[a] (%)
1	**Fe-POP-1** (1.0)	DMF	23
2	**Fe-POP-2** (1.0)	DMF	53
3	**Fe-POP-3** (1.0)	DMF	85
4	**Fe-POP-3** (2.5)	DMF	82
5	**Fe-POP-3** (0.5)	DMF	76
6	**Fe-POP-3** (1.0)	THF	80
7	**Fe-POP-3** (1.0)	^{i}PrOH	41
8	**2b** (1.0)	DMF	83
9	**2c** (1.0)	DMF	<1
10	**2b** (1.0)	^{i}PrOH	21
11	**2c** (1.0)	^{i}PrOH	7

[a] Yield determined by GC using *n*-dodecane as the internal standard.
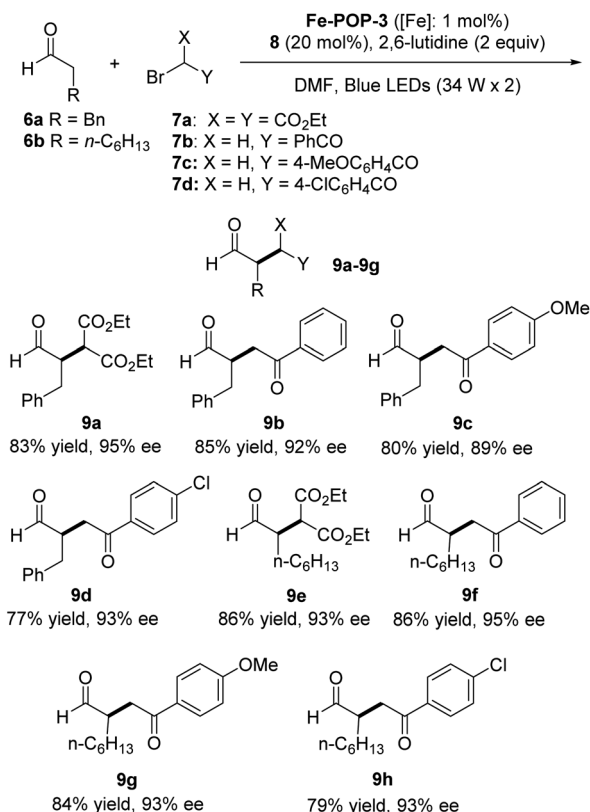
Scheme 4 Substrate scope of **Fe-POP-3**-catalyzed enantioselective α-alkylation of aldehydes **6a–b** for the formation of the corresponding products **9a–h**. The yield represents the isolated one. The reactions were carried out on the scale of 1 mmol of **6** (**7**: (0.5 mmol) in DMF (1 mL)).

This journal is © The Royal Society of Chemistry 2021

J. Mater. Chem. A, 2021, **9**, 6361–6367 | **6365**

bromoacetophenones **7b–d** (Scheme 4). All the reactions afforded the corresponding coupling products **9b–h** in good to excellent yields (77–86%) and ee values (89–93%), which were comparable to or even higher than those of the identical reaction catalyzed homogeneously by Fe(bpy)$_3$Br$_2$.[33] Moreover, the introduction of electron-donating (MeO) or withdrawing (Cl) groups on the benzene ring did not have great influence on both yield and enantioselectivity, which reflected a good tolerance of the variety of substrates. The mechanism for the homogeneous photocatalysis of the above reactions by Fe(bpy)$_3$Br$_2$ has been established by Ceroni and Cozzi.[33] It is reasonable to propose that the present heterogeneous photocatalysis of these reactions should proceed through an identical mechanism (Fig. S16, ESI†).

Given the high yield and enantioselectivity of **9a** from the reaction of **6a** and **7a** under the heterogeneous photocatalysis of **Fe-POP-1**, we further studied the recyclability of **Fe-POP-1** for this transformation. After 10 times of repeated use, **Fe-POP-1** still enabled the production of **9a** in 62% yield, even though the yield gradually decreased with the repeated use of the catalyst (Fig. 4b). Notably, even after 10 times recycling, the ee value was just decreased slightly from the original 95% to 91%. This result clearly reflected the high stability of the heterogeneous photocatalyst and also suggested that the decrease of the yield was caused mainly by the loss of the catalyst during the processes.

Conclusions

We have demonstrated a convenient strategy for the preparation of Fe(bpy)$_3$-based porous organic polymers. The new earth-abundant metal complex-derived materials work well as heterogeneous photocatalysts for recyclable organic transformations. For the two investigated reactions, the heterogeneous photocatalysts exhibited high activity that rivals or even surpasses that of homogeneous control photocatalysts. Moreover, the enantioselectivity of the coupling reactions mediated by the chiral co-organocatalyst also rivals that obtained under the homogeneous reaction conditions, which illustrates the high stability of the new kind of metal complex-derived porous polymer. This work opens new perspectives for the use of other earth-abundant metal complexes for efficient heterogeneous photocatalysis of organic transformations.

Conflicts of interest

There are no conflicts to declare.

Acknowledgements

Notes and references

1 C. K. Prier, D. A. Rankic and D. W. C. MacMillan, *Chem. Rev.*, 2013, **113**, 5322–5363.

2 J. M. R. Narayanam and C. R. J. Stephenson, *Chem. Soc. Rev.*, 2011, **40**, 102–113.

3 D. M. Schultz and T. P. Yoon, *Science*, 2014, **343**, 985.

4 J. Xuan and W.-J. Xiao, *Angew. Chem., Int. Ed.*, 2012, **51**, 6828–6838.

5 R. Brimioulle, D. Lenhart, M. M. Maturi and T. Bach, *Angew. Chem., Int. Ed.*, 2015, **54**, 3872–3890.

6 X. Huang and E. Meggers, *Acc. Chem. Res.*, 2019, **52**, 833–847.

7 H. Zhang and S. Yu, *Acta Chim. Sin.*, 2019, **77**, 832–840.

8 X.-Y. Yu, Q.-Q. Zhao, J. Chen, W.-J. Xiao and J.-R. Chen, *Acc. Chem. Res.*, 2020, **53**, 1066–1083.

9 H.-H. Zhang, H. Chen, C.-J. Zhu and S.-Y. Yu, *Sci. China: Chem.*, 2020, **63**, 637–647.

10 S. K. Pagire, T. Foell and O. Reiser, *Acc. Chem. Res.*, 2020, **53**, 782–791.

11 J. M. Lee and A. I. Cooper, *Chem. Rev.*, 2020, **120**, 2171–2214.

12 P. Xu, W.-P. Li, J. Xie and C.-J. Zhu, *Acc. Chem. Res.*, 2018, **51**, 484–495.

13 F. Teplý, *Collect. Czech. Chem. Commun.*, 2011, **76**, 859–917.

14 D. Ravelli and M. Fagnoni, *ChemCatChem*, 2012, **4**, 169–171.

15 M. Majek and A. J. Wangelin, *Acc. Chem. Res.*, 2016, **49**, 2316–2327.

16 M. K. Bogdos, E. Pinard and J. A. Murphy, *Beilstein J. Org. Chem.*, 2018, **14**, 2035–2064.

17 R. Li, J. Byun, W. Huang, C. Ayed, L. Wang and K. A. I. Zhang, *ACS Catal.*, 2018, **8**, 4735–4750.

18 Y. Markushyna, C. A. Smith and A. Savateev, *Eur. J. Org. Chem.*, 2020, **2020**, 1294–1309.

19 B. Chen, L.-Z. Wu and C. H. Tung, *Acc. Chem. Res.*, 2018, **51**, 2512–2523.

20 Q. Liu and L.-Z. Wu, *Natl. Sci. Rev.*, 2017, **4**, 359–380.

21 C. B. Larsen and O. S. Wenger, *Chem.–Eur. J.*, 2018, **24**, 2039–2058.

22 J. K. McCusker, *Science*, 2019, **363**, 484–488.

23 J.-L. Dai, W.-L. Liu and Q. Liu, *Acta Chim. Sin.*, 2019, **77**, 911–915.

24 T. Mandal, S. Das and S. De Sarkar, *Adv. Synth. Catal.*, 2019, **361**, 3200–3209.

25 A. Hossain, A. Bhattacharyya and O. Reiser, *Science*, 2019, **364**, eaav9713.

26 W.-M. Cheng and R. Shang, *ACS Catal.*, 2020, **10**, 9170–9196.

27 B. M. Hockin, C. Li, N. Robertson and E. Zysman-Colman, *Catal. Sci. Technol.*, 2019, **9**, 889–915.

28 O. S. Wenger, *J. Am. Chem. Soc.*, 2018, **140**, 13522–13533.

29 M. D. Woodhouse and J. K. McCusker, *J. Am. Chem. Soc.*, 2020, **142**, 16229–16233.

30 O. S. Wenger, *Chem.–Eur. J.*, 2019, **25**, 6043–6052.

31 W.-J. Zhou, X.-D. Wu, M. Miao, Z.-H. Wang, L. Chen, S.-Y. Shan, G.-M. Cao and D.-G. Yu, *Chem.–Eur. J.*, 2020, **26**, 15052–15064.

32 J.-H. Ye, M. Miao, H. Huang, S.-S. Yan, Z.-B. Yin, W.-J. Zhou and D.-G. Yu, *Angew. Chem., Int. Ed.*, 2017, **56**, 15416–15420.

33 A. Gualandi, M. Marchini, L. Mengozzi, M. Natali, M. Lucarini, P. Ceroni and P. G. Cozzi, *ACS Catal.*, 2015, **5**, 5927–5931.

34 S. Parisien-Collette, A. C. Hernandez-Perez and S. K. Collins, *Org. Lett.*, 2016, **18**, 4994–4997.

6366 | *J. Mater. Chem. A*, 2021, **9**, 6361–6367

This journal is © The Royal Society of Chemistry 2021

35 Y. H. Cho, J. H. Kim, H. An, K.-H. Ahn and E. J. Kang, *Adv. Synth. Catal.*, 2020, **362**, 2183–2188.

36 J. Y. Hwang, A. Y. Ji, S. H. Lee and E. J. Kang, *Org. Lett.*, 2020, **22**, 16–21.

37 Q. Sun, B. Aguila, Y. Song and S. Ma, *Acc. Chem. Res.*, 2020, **53**, 812–821.

38 T.-X. Wang, H.-P. Liang, D. A. Anito, X. Ding and B.-H. Han, *J. Mater. Chem. A*, 2020, **8**, 7003–7034.

39 T. Zhang, G. Xing, W. Chen and L. Chen, *Mater. Chem. Front.*, 2020, **4**, 332–353.

40 C. Xu, W.-J. Zhang, J.-T. Tang, C.-Y. Pan and G.-P. Yu, *Front. Chem.*, 2018, **6**, 592.

41 Y. Byun, S. H. Je, S. N. Talapaneni and A. Coskun, *Chem.–Eur. J.*, 2019, **25**, 10262–10283.

42 R.-R. Liang and X. Zhao, *Org. Chem. Front.*, 2018, **5**, 3341–3356.

43 P. Kaur, J. T. Hupp and S. T. Nguyen, *ACS Catal.*, 2011, **1**, 819–835.

44 Y.-G. Zhang and S. N. Riduan, *Chem. Soc. Rev.*, 2012, **41**, 2083–2094.

45 B. Yang, H. Wang, D.-W. Zhang and Z.-T. Li, *Chin. J. Chem.*, 2020, **38**, 970–980.

46 J.-L. Wang, C. Wang, K. E. deKrafft and W.-B. Lin, *ACS Catal.*, 2012, **2**, 417–424.

47 L.-Y. Li, C.-Y. Cui, W.-Y. Su, Y.-X. Wang and R.-H. Wang, *Nano Res.*, 2016, **9**, 779–786.

48 Y.-P. Wu, M. Yan, Z.-Z. Gao, J.-L. Hou, H. Wang, D.-W. Zhang and Z.-T. Li, *Chin. Chem. Lett.*, 2019, **30**, 1383–1386.

49 X.-J. Yang, T. Liang, J.-X. Sun, M. J. Zaworotko, Y. Chen, P. Cheng and Z.-J. Zhang, *ACS Catal.*, 2019, **9**, 7486–7493.

50 Y. Luo, Z.-Y. Xu, H. Wang, X.-W. Sun, Z.-T. Li and D.-W. Zhang, *ACS Macro Lett.*, 2020, **9**, 90–95.

51 Z.-G. Xie, C. Wang, K. E. deKrafft and W.-B. Lin, *J. Am. Chem. Soc.*, 2011, **133**, 2056–2059.

52 H.-P. Liang, Q. Chen and B.-H. Han, *ACS Catal.*, 2018, **8**, 5313–5322.

53 C. Wang, Z.-G. Xie, K. E. deKrafft and W.-B. Lin, *ACS Appl. Mater. Interfaces*, 2012, **4**, 2288–2294.

54 Z.-Z. Gao, Y.-Y. Xu, Z.-K. Wang, H. Wang, D.-W. Zhang and Z.-T. Li, *ACS Appl. Polym. Mater.*, 2020, **2**(11), 4885–4892.

55 Z.-Y. Xu, Y. Luo, D.-W. Zhang, H. Wang, X.-W. Sun and Z.-T. Li, *Green Chem.*, 2020, **22**, 136–143.

56 R. Dorta, R. Goikhman and D. Milstein, *Organometallics*, 2003, **22**, 2806–2809.

57 X.-F. Li, X.-B. Liu, J.-Y. Chao, Z.-K. Wang, F.-U. Rahman, H. Wang, D.-W. Zhang, Y. Liu and Z.-T. Li, *Sci. China: Chem.*, 2019, **62**, 1634–1638.

58 Y.-J. Su, L.-R. Zhang and N. Jiao, *Org. Lett.*, 2011, **13**, 2168–2171.

59 X.-J. Yang, T. Liang, J.-X. Sun, M. J. Zaworotko, Y. Chen, P. Cheng and Z.-J. Zhang, *ACS Catal.*, 2019, **9**, 7486–7493.

60 D. A. Nicewicz and D. W. C. Macmillan, *Science*, 2008, **322**, 77–80.

This journal is © The Royal Society of Chemistry 2021

J. Mater. Chem. A, 2021, **9**, 6361–6367 | **6367**